

RESEARCH ARTICLE

Engineering

Operation of DC Motor with Multi-Level Inverter in PWAM Method

Operación de un Motor DC con Invertidor Multi-Nivel Mediante el Método PWAM

Erol Can  ^{1*}

¹ Department of Aviation Electric-Electronics, School of Civil Aviation, Erzincan Binali Yıldırım University, Erzincan, Turkey.

Correspondence

Erol Can, Erzincan University-Turkey.
Email: cn_e@hotmail.com

Copyright : Licencia de Creative Commons Reconocimiento-NoComercial 4.0 Interna.



The publication of this journal is funded by Universidad ECCI, Bogotá-Colombia.

Editors: Robert Paul Salazar

Editorial assistant : Luz Adriana Suárez Suárez.

How to cite: Erol Can, **Operation of DC Motor with Multi-Level Inverter in PWAM Method**, TECCIENCIA, Vol. 16, No. 30, 1-14, 2021

DOI:<http://dx.doi.org/10.18180/tecciencia.2021.30.1>

Resumen

El control de motores de DC con métodos de conmutación es un dispositivo interesante con muchas aplicaciones prácticas. Un convertidor reductor-elevador DC-DC es uno de los métodos utilizados para operar el motor DC. Aunque el convertidor reductor-elevador de CC para aplicaciones de motores de CC se ha estudiado ampliamente, tiene algunas desventajas. En este estudio, la estructura del inversor multinivel que es

ABSTRACT

DC motor control with switching methods is an interesting device with many practical applications. A DC-DC buck-boost converter is one of the methods used to operate the DC motor. Although the DC buck-boost converter for dc motor applications has been widely studied, they have some handicaps. In this study, the multi-level inverter structure that is different from the methods of DC motor driving is used to drive the DC motor. There will be no passive elements in the proposed circuit although the dc-dc converters have passive elements. So, while the inadequacies for the loads needing high current will be eliminated, the handicaps of the switching can be avoided. Current, torque, and voltage on the load will also be created by Pulse Width Amplitude Method (PWAM). As a different from other Pulse width modulation methods (PWM); the torque, current, and voltage of the motor can be controlled with PWAM in the horizontal and vertical axes. In the design stage; inverter switch structure and operation are given after the method of produced PWMs introduced. The equations of the voltages that will occur in the loads are created according to the working structure of the switches. DC motor structure is also given. In the simulation stage; Continuous and discontinuous modes of the proposed circuit are performed. Then torque of dc motor, armature current and speed are tested according to switching at different frequencies and different modulation indices.

keywords: PWAM, continuous mode, discontinuous mode.

* Equally contributing authors.

diferente de los métodos de conducción del motor de CC se utiliza para impulsar el motor de DC. No habrá elementos pasivos en el circuito propuesto aunque los convertidores dc-dc tienen elementos pasivos. Por lo tanto, mientras se eliminarán las deficiencias para las cargas que necesitan alta corriente, se pueden evitar las desventajas de la conmutación. La corriente, el par y el voltaje en la carga también serán creados por el Método de Amplitud de Ancho de Pulso (PWAM). A diferencia de otros métodos de modulación de ancho de pulso (PWM); el par, la corriente y el voltaje del motor se pueden controlar con PWAM en los ejes horizontal y vertical. En la etapa de diseño; La estructura y operación del interruptor inversor se dan después del método de PWM producido introducido. Las ecuaciones de los voltajes que ocurrirán en las cargas se crean de acuerdo con la estructura de trabajo de los interruptores. También se da la estructura del motor de DC. En la etapa de simulación; Se realizan modos continuos y discontinuos del circuito propuesto. Luego, el par del motor de DC, la corriente de armadura y la velocidad se prueban de acuerdo con la conmutación a diferentes frecuencias y diferentes índices de modulación.

keywords: PWAM, métodos continuos, métodos discontinuos.

1 | INTRODUCTION

DC motors are one of the machines where DC energy is applied and generate mechanical power. Torque/speed compatibility with many mechanical loads is a basic feature of the DC motor [1]. At the same time, methods of controlling the main parameters of the DC motor such as speed, torque are simpler and cheaper than controlling the main parameters of other motors [2, 3, 4]. A DC-DC buck-boost converter is one of the methods used to operate the dc motor [5]. These dc-dc converters are controlled by pulse width modulation [6, 7, 8, 9]. PID, fuzzy logic and open-loop are used as control methods of these dc-dc converters [10, 11, 12]. These dc-dc converters have many passive elements such as capacitors, coils, and diodes [9, 13, 14]. The switching times and passive elements of the circuit can be inadequate in energy management for low impedance loads. However, in some applications requiring high current, some handicaps arise while applying welding power from zero to maximum for load. DC source control has performed with the Pulse Width Modulation method for the dc motor in [15]. However, in this method, the current, torque, and voltage PWMs on the load decrease to zero at the end of the working time, and the discontinuous mode operates because there is no dc-dc converter in the system. With the proposed method, the current, torque, and voltage on the load never drop to zero in continuous mode, although there are no dc converters in the system. Different from some studies in [16, 17, 18, 19]; the current, torque, and voltage on the load can also be controlled with amplitudes in the time axis. So, the multi-level inverter structure used to drive alternating loads in some studies in [20, 21, 22] is used for the first time to drive dc motor in this study. At the same time, when this inverter structure is used, the proposed circuit will not have passive elements used by converters, insufficiencies such as insulation, high heating, and coil effect in driving loads that require high current will be eliminated. Then, the strain on the switch will be prevented. Current, torque, and voltage on the load will be created by Pulse Width Amplitude Method (PWAM). In this method, because PWM provides the width of the pulse on the load, it is creating a voltage on the load at the switching source levels. In case a higher level of voltage is applied to the load, the multi-level inverter structure ensures that the voltage amplitude is increased on the load. Different PWMs are produced within the time periods other than the main PWMs' operating times. The duration of these PWMs is less than the main PWMs, and constant operation of the fixed source is ensured with these PWMs. Thus, while the DC motor's continuous mode operation is also ensured, the current torque and voltage on the load never drop to zero. In Section 2; after the method of produced PWMs, inverter switch structure and operation are given, the equations of the voltages that will occur in the loads are created according to the working structure of the switches. DC motor structure is also given. In Section 3; Continuous mode and discontinuous mode of the proposed circuit are performed. In the simulations; Torque of DC motor armature current and speed are tested according to different frequencies switching and different modulation indexes. When the obtained results are observed, dc motor torque, current, and speed are controlled in the desired way by using the new method in continuous and discontinuous mode.

2 | DESIGN OF THE PROPOSED METHOD

Fig. 1 Demonstrates circuit structure at discontinuous voltage mode for periods. The circuit structure includes 3 sources and 8 IGBT switches for discontinuous mode. Fig. 2-(a) also shows the operating mode when the inverter generates an alternating voltage Table 1 shows the working order of the elements.

TABLE 1 Working order of the elements.

ANGLE	$0^0 - 60^0$	$60^0 - 120^0$	$120^0 - 180^0$	$180^0 - 240^0$	$240^0 - 300^0$	$270^0 - 360^0$
IGBT0	1	0	1	0	0	0
IGBT1	0	1	0	0	0	0
IGBT2	1	0	1	0	0	0
IGBT3	0	0	0	1	0	1
IGBT4	0	0	0	0	1	0
IGBT5	0	0	0	1	0	1
IGBT7	1	1	1	1	1	1
DCV0	1	1	1	1	1	1
DCV1	1	0	1	1	0	1
DCV2	0	1	0	0	1	0
DC MOTOR	1	1	1	1	1	1

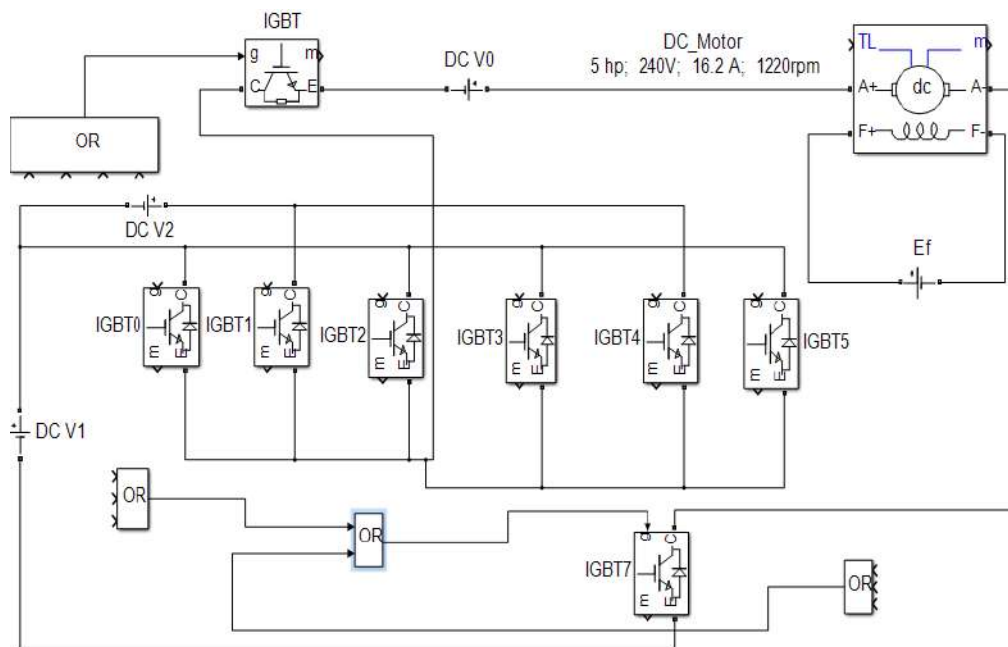


FIG. 1 Circuit structure for discontinuous voltage mode for periods.

In Fig. 2-(b) the inverter shows the operating mode while generating Direct Voltage. While the V source is considered for the first level voltage in Fig. 2-(a), the source used for the second level can be considered as 2V. \mathcal{D} is working ratio of pulse width modulation; $(1 - \mathcal{D})$ for PWM is nonworking times. T is the time period.

The general structure of the voltage that will occur for loads is found in equations as follows

$$V_L = \frac{4V}{3} \mathcal{D}T \quad \text{voltage structure.} \quad (1)$$

With this voltage structure, the load will work in discontinuous voltage mode. The voltage will decrease to zero for each pulse. An extra switch is added to the third source to operate in continuous voltage mode for periods when PWMs for discontinuous voltage mode do not control the load, and the circuit can be rearranged as in Fig. 4. We show in Fig. 3 the load voltage generated by the PWMs for the continuous operation mode.

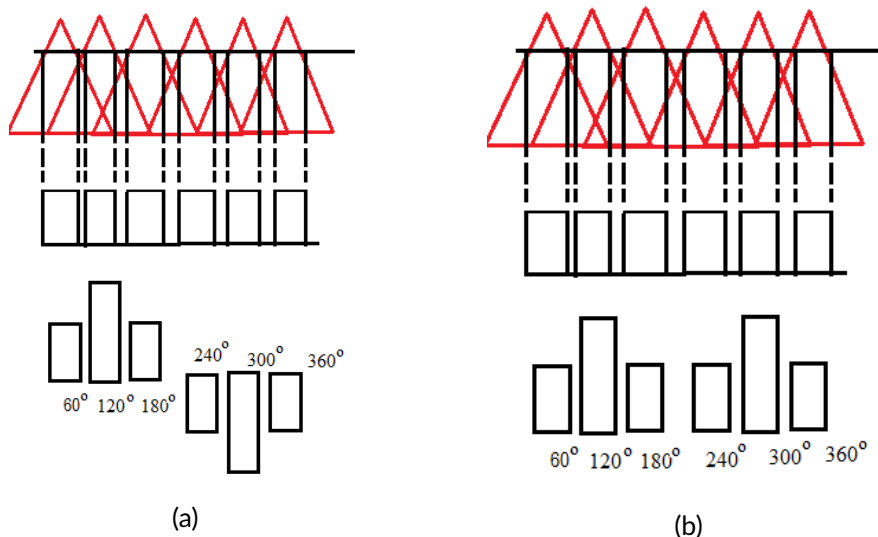


FIG. 2 a) For PWM, the inverter generating an alternating voltage b) for PWM, the inverter operating DC motor at discontinues.

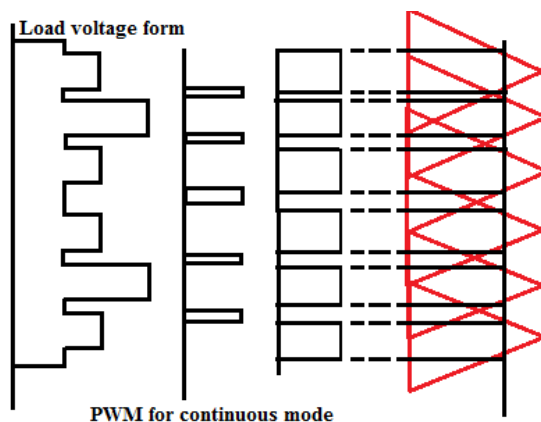


FIG. 3 The load voltage generated by the PWMs for the continuous operation mode.

The circuit arranged in Fig. 4 is operated with the PWMs in Fig. 3. In this embodiment, the discontinuous mode PWMs operate all switches while the continuous mode PWMs only operate the VDC0 source. In this case, the voltage on the load is prevented from being zero. Load voltage equations are rearranged as below equations when V for VDC0 is considered

$$V_L = \frac{7V\mathcal{D} + V}{6}. \quad (2)$$

This is the first time that a multi-level inverter will control the DC motor. The model of DC motor in Matlab Simulink is as given in Fig. 5. The mathematical model of the applied DC motor belongs to the external excited DC machine application. The model has some parameters. The resistance of armature is R_a in ohms; Armature of inductance is L_a in Henry. Field of resistance R_f in ohms. Field inductance is L_f in Henry. The

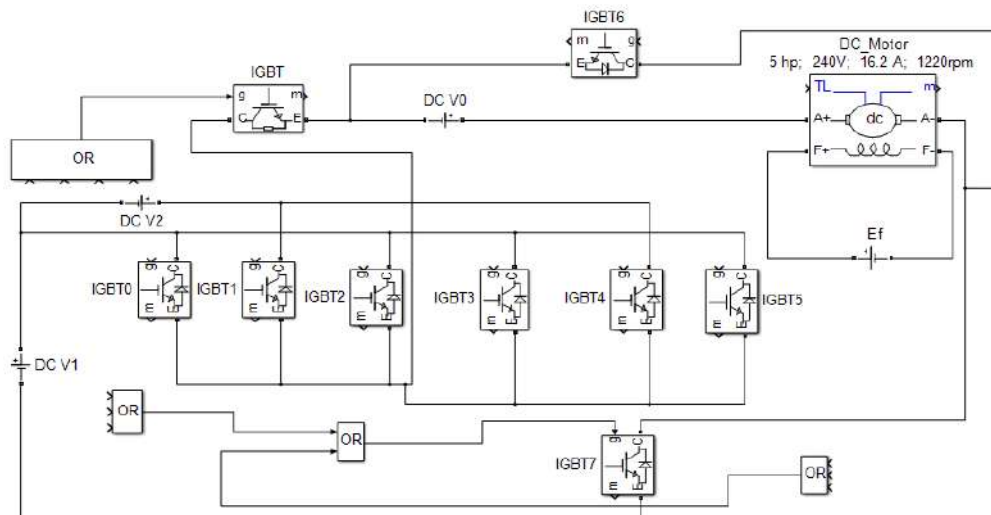


FIG. 4 Circuit structure for continuous voltage mode for periods.

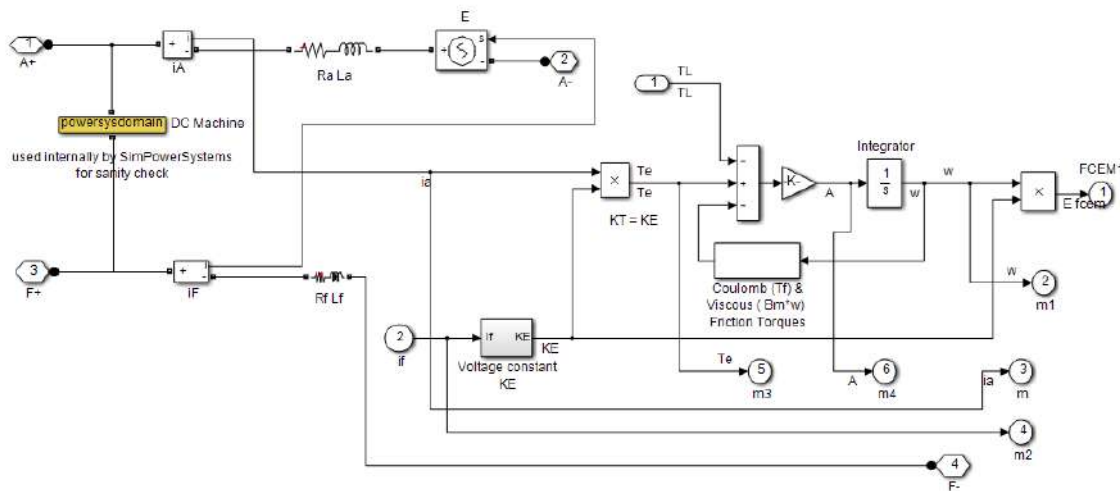


FIG. 5 The model of DC motor in Matlab Simulink.

mutual inductance of field armature L_{af} in Henry. The total inertia for the DC machine is J in $kg \cdot m^2$. The total friction coefficient of the DC machine is B_m in Nm . The total Coulomb for friction torque constant of the DC machine is T_f in Nm . K_E is voltage constant in volt; w is speed for the machine in rad / s and rpm . Armature current is i_a in ampere; T_e is electrical torque as in Nm ; The current for the field is i_f at ampere. It was obtained by a serial connection of the field terminal + F, -F between R_f and L_f . The armature circuit has been obtained between + A and -A by the series connection of R_a and L_a , and the electromotor force E , which is modeled

in series with this circuit, is expressed as in Eq. (3) given by

$$E = K_E w. \quad (3)$$

Considering the PWM's working times and the principle of operation of the proposed drive system according to discontinuous mode Eq. (3) can be arranged as in Eq. (4) again

$$E = \frac{K_E w}{3} \mathcal{D}. \quad (4)$$

Considering the PWM's working times and the principle of operation of the proposed drive system according to discontinuous mode Eq. (3) can be arranged as in Eq. (5) as follows

$$E = \frac{K_E w}{3} (7\mathcal{D} + 1) \quad (5)$$

where K_E is proportional to the field current i_f in an externally excited DC machine model. The parameter K_E can be described as in the following equation

$$K_E = L_{af} i_j. \quad (6)$$

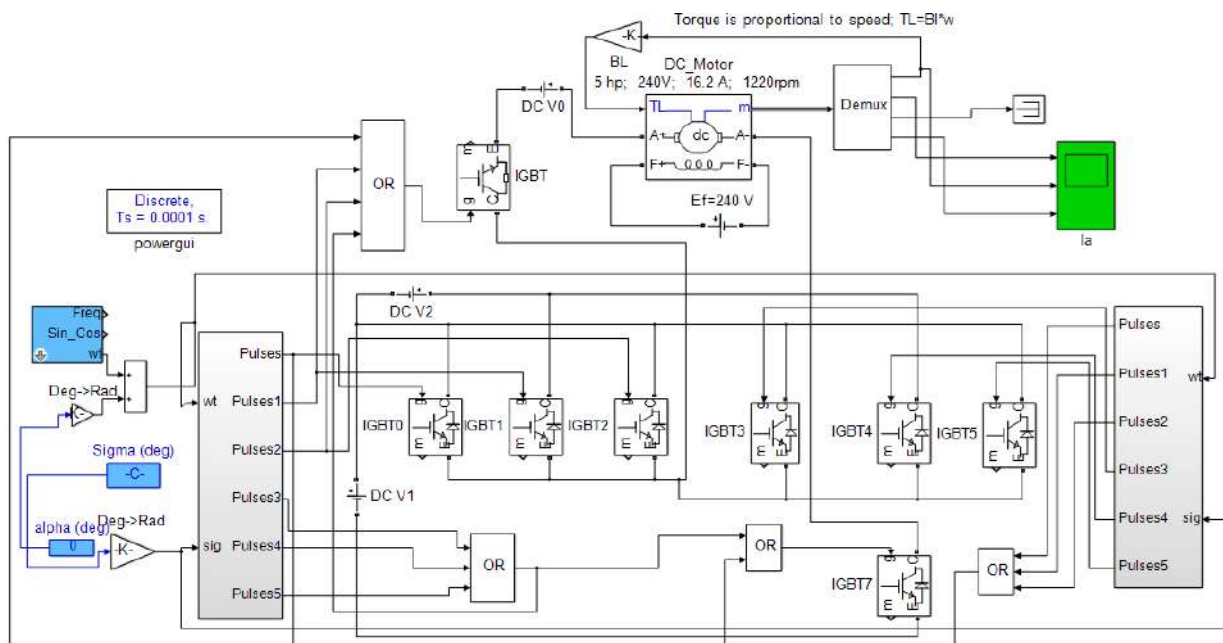


FIG. 6 The Matlab Simulink circuit model of the DC motor in discontinuous mode.

For machine speed w , the following equations are used

$$\frac{j}{B_m} \frac{dw}{dt} - w = T_e - T_L - T_f \quad (7)$$

and

$$\dot{\omega} = \frac{T_e - T_L - T_f}{j_s - B_m}. \quad (8)$$

3 | APPLICATION OF THE PROPOSED METHOD

At this stage, the operation of the proposed method in discontinuous and discontinuous mode will be tested on the DC motor. Fig. 6 shows the Matlab Simulink circuit model of the DC motor that will operate in discontinuous mode.

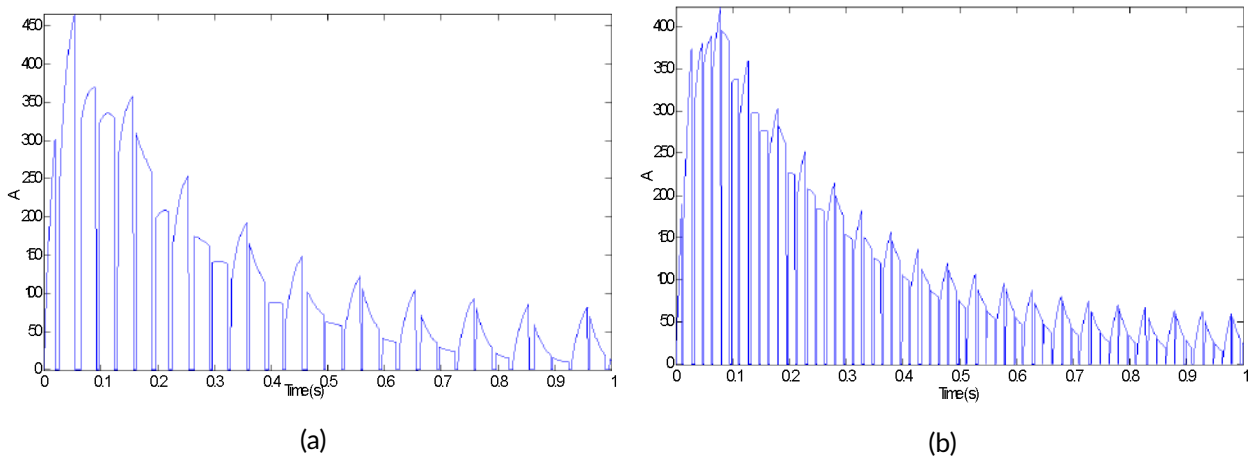


FIG. 7 a) DC motor current for 0.033 s of switching time, b) DC motor current for 0.015 s of switching time.

When the circuit in Fig. 6 is operated at different switching times, the currents formed on the DC motor are as shown in in Figs. 7 and 8.

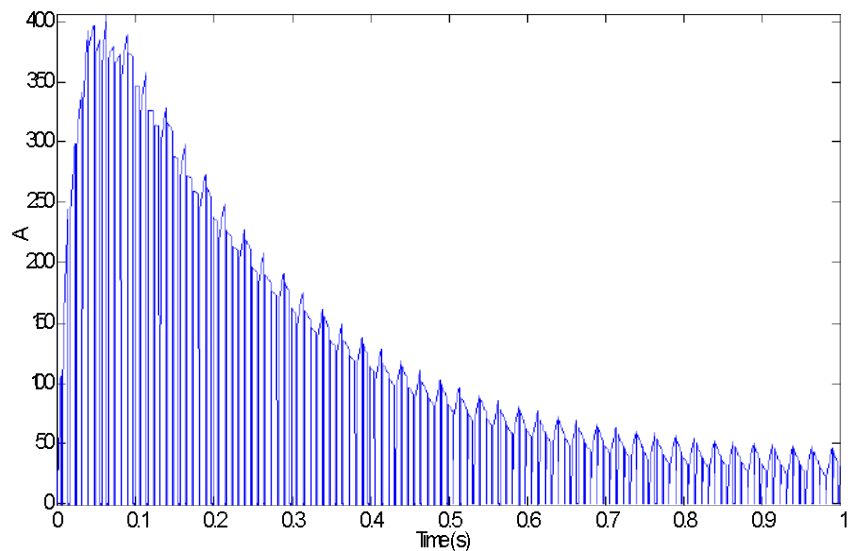


FIG. 8 DC motor current for 0.007 s of switching time.

As the switching times increase, the number of PWMs dividing the current increases. DC motor current can

be controlled both with PWM amplitudes and widths. The current value of the DC motor reaches a maximum value that is 475 A for 0.033 switching time. The current value reaches a maximum value that is 450 A. for 0.015 switching time. The current value of the DC motor reaches a maximum value that is 475 A for 0.007 switching time. After the circuit in Fig. 6 is operated at three different switching times, the speed on the DC motor are as shown in Fig. 9 and Fig. 10.

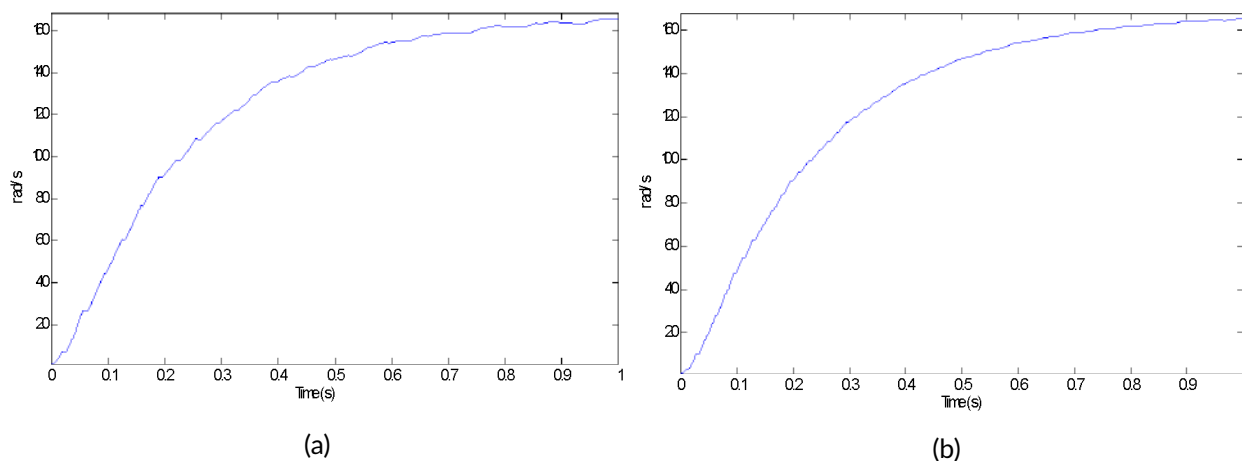


FIG. 9 a) DC motor current for 0.033s of switching time, b) DC motor current for 0.015s of switching time.

DC motor speed is 165 rad/s in 3 different switching times. It is observed that the oscillations in acceleration decrease as the switching times increase. When the circuit in Fig. 6 is operated at different switching times, the torques formed on the DC motor are as shown in Figs. 11 and 13.

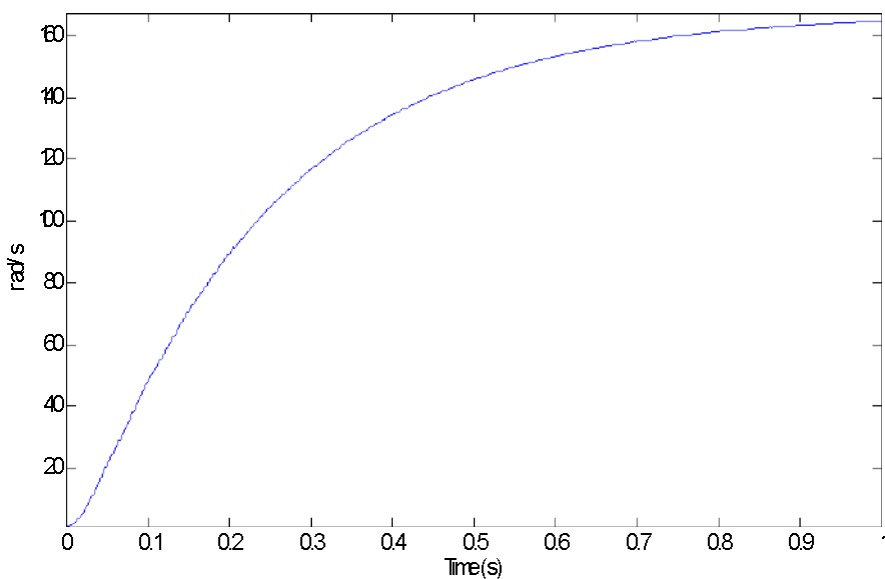


FIG. 10 DC motor current for 0.007s of switching time.

As the switching times increase, the number of PWMs dividing the torque increases. DC motor torque can be controlled both with PWM amplitudes and widths. The torque value of the DC motor reaches a maximum value that is 850Nm for 0.033 switching time. The torque value reaches a maximum value that is 800 Nm for 0.015 switching time. The torque value of the DC motor reaches a maximum value that is 750 Nm for 0.007 switching time. After Dc motor is tested at discontinues mode, it performs at continues mode. Fig. 12 shows

the Matlab Simulink circuit model of the DC motor that will operate in continuous mode.

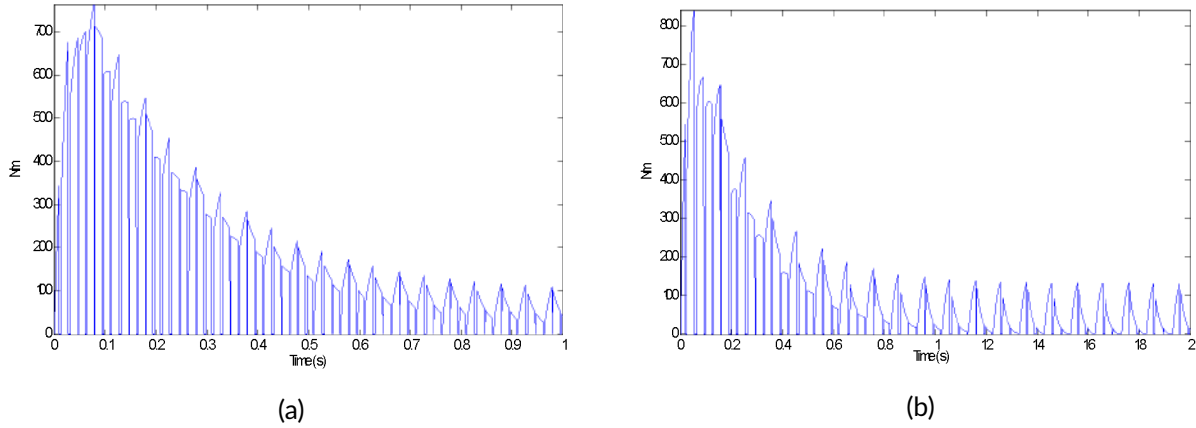


FIG. 11 a) DC motor torque for 0.015s of switching time, b) DC motor torque for 0.033s of switching time.

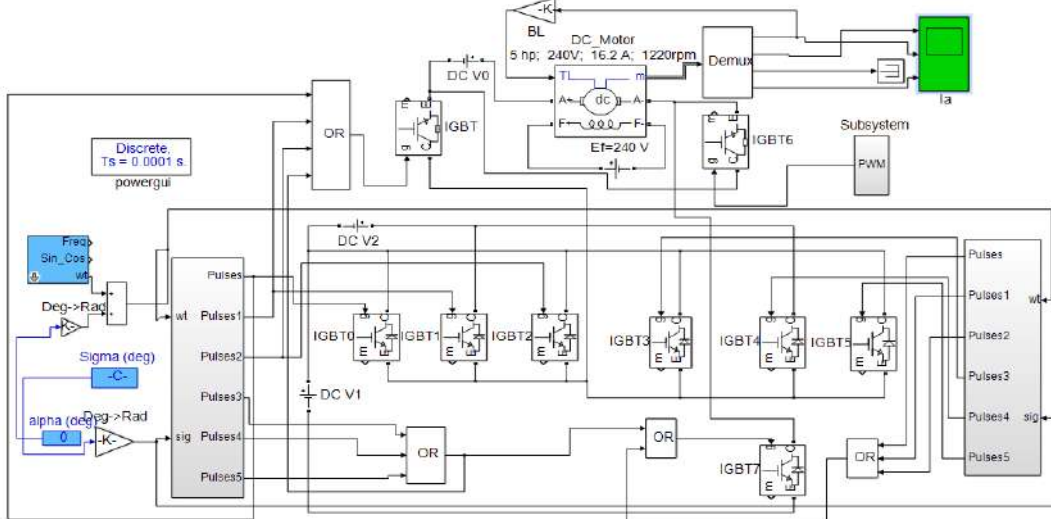


FIG. 12 the circuit model of Matlab Simulink for the DC motor operating in continuous mode.

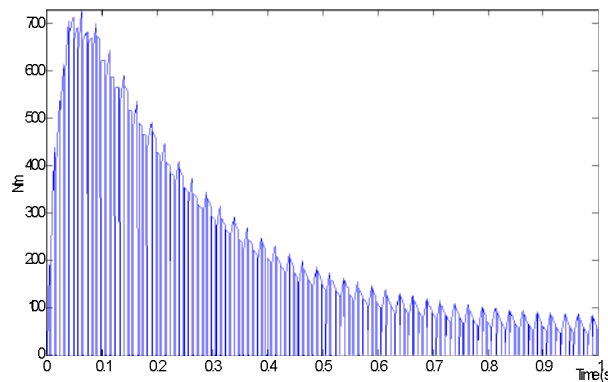


FIG. 13 DC motor current for 0.007s of switching time.

Unlike the discontinuous mode state, when the VDC 0 source is operated also with PWMs of continuous mode, the torque and current values never decrease to zero. When the circuit switches in Fig. 12 are operated with the switching time at 0.007s, the resulting motor currents are in Fig. 14-(a), the engine speeds that occur as in Fig. 1-(b). The engine torques that occur as in Fig. 15.

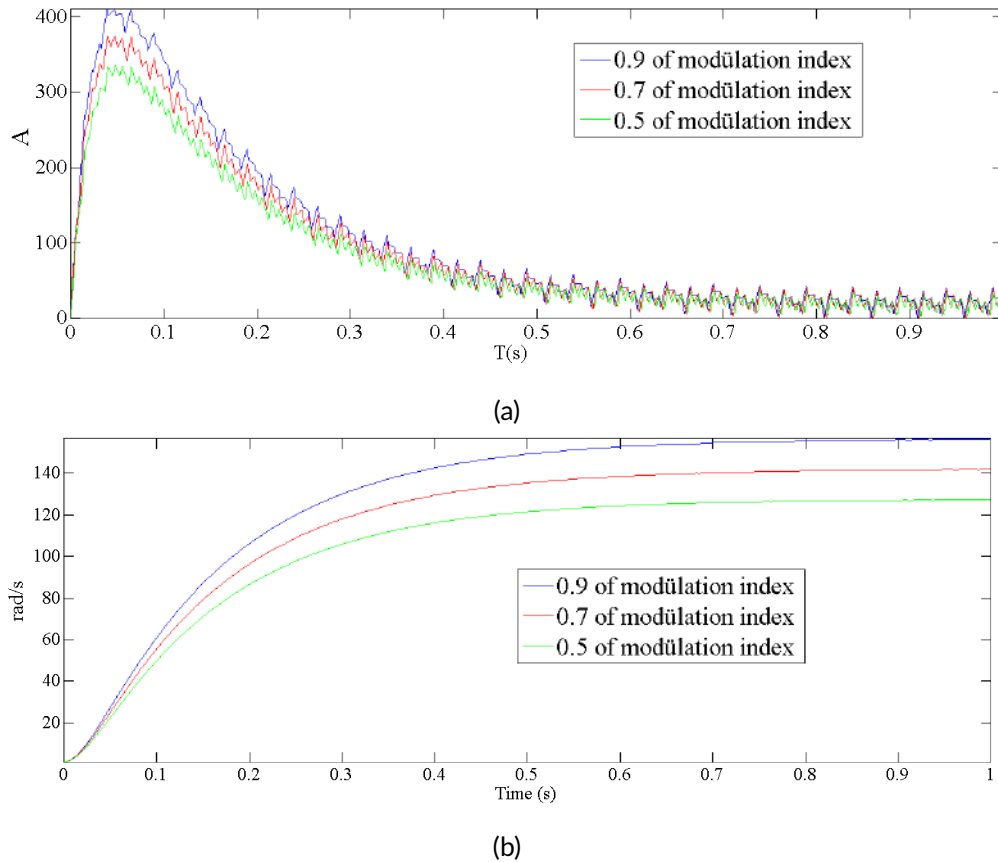


FIG. 14 a) Motor currents for continues mode b) motor speeds for continues mode.

Fig. 14 show dc motor currents and speeds in 3 different modulation indexes. In the 0.9 modulation index, the motor current reaches a maximum value of 450 A at 0.07 s, while the motor speed reaches 165 rad / s in 1 s. In the 0.7 modulation index, the motor current reaches a maximum value of 375 A at 0.06 s, while the motor speed reaches 142 rad / s in 1 s. In the 0.5 modulation index, the motor current reaches a maximum value of 330 A at 0.05 s, while the motor speed reaches 127 rad/s in 1s.

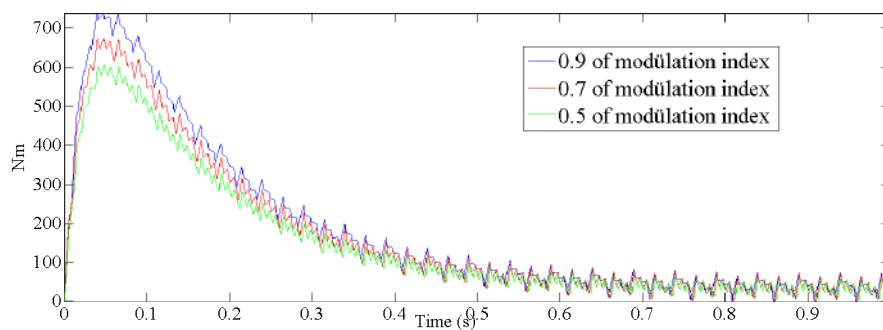


FIG. 15 Motor torques for continues mode.

Motor torques in three different modulation indexes are given in Fig. 15. In the 0.9 modulation index, the engine torque reaches 750Nm at 0.07s, while the maximum engine speed reaches 165 rad / s. In the 0.7 modulation index, the engine torque reaches 675Nm at 0.06s, while the maximum engine speed reaches 142 rad / s. In the 0.5 modulation index, maximum value of the engine torque reaches 600Nm at 0.05s, while the maximum engine speed reaches 127 rad / s. The current values of the DC motor for five different modulation indexes are given in Fig. 16.

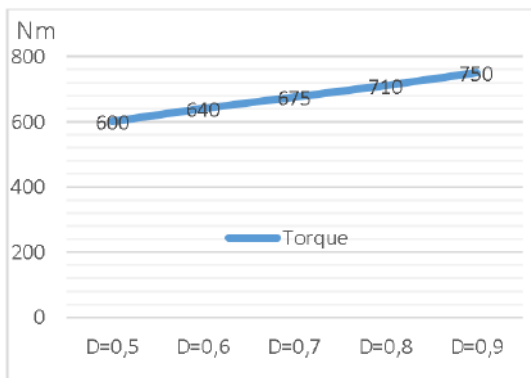


FIG. 16 The armature current values for five different modulation indices.

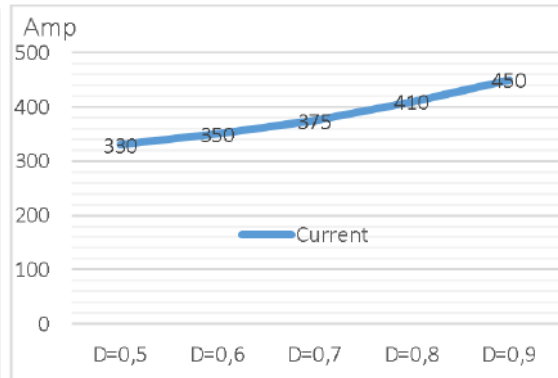


FIG. 17 The armature torque values for five different modulation indices.

The maximum values of torque increase linearly with the increase of modulation index. While it is 640 Nm in the 0.6 modulation index, it is 710 Nm in the 0.8 modulation index. The speed values of the DC motor for five different modulation indexes are given in Fig. 18.

The maximum values of armature current increase linearly with the increase of modulation index. While it is 350 A in the 0.6 modulation index, it is 410 A in the 0.8 modulation index. The torque values of the DC motor for five different modulation indexes are given in Fig. 17.

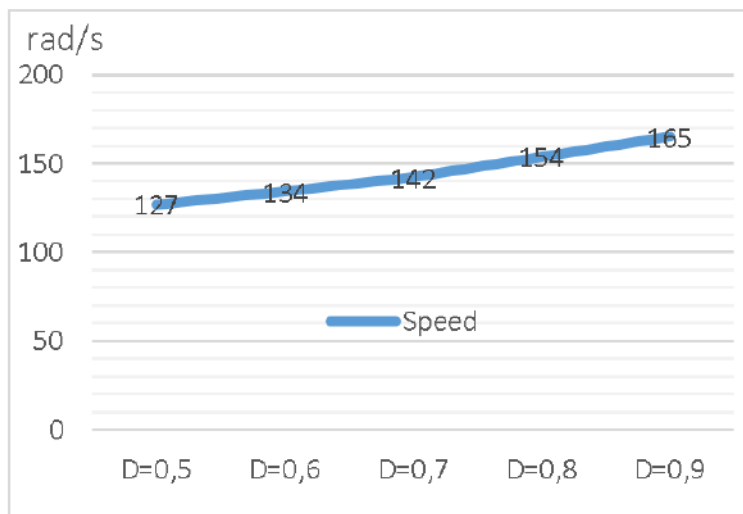


FIG. 18 The speed values of DC motor for five different modulation indices.

The maximum values of torque increase linearly with the increase of modulation index. While it is 134 rad/s in the 0.6 modulation index, it is 154 rad/s in the 0.8 modulation index. DC-DC converters are controlled by increasing and decreasing the DC voltage on load. However, it is difficult to control the full power of the source from 0 to the maximum by means of switches on the load. In this study, the DC source voltage value is

controlled in width and amplitude, and the entire power of the source can be controlled from 0 to maximum load via switches. According to the results obtained; the speed, current, and torque of the dc motor can be changed effectively by changing the working times of the PWMs.

4 | CONCLUSIONS

When this inverter structure was used, there would be no passive elements in proposed circuit although there were in the dc-dc converters and while the inadequacies for the loads requiring high current would be eliminated and the handicaps of the switch will be avoided. Current, torque, and voltage on the load will be created by Pulse Width Amplitude Method (PWAM). Design stage; after the Method of produced PWMs, inverter switch structure and operation are given, the equations of the voltages that will occur in the loads are created according to the working structure of the switches. DC motor structure is also given. In the simulation stage; Continuous mode and discontinuous mode of the proposed circuit is performed. Then torque of dc motor Armature current and speed are tested according to different frequencies switching and different modulation indexes. The torque value of the DC motor at discontinuous mode reached a maximum value that was 850Nm for 0.033 switching time. The torque value reached a maximum value that was 800 Nm for 0.015 switching time. The torque value of the DC motor reached a maximum value that was 750 Nm for 0.007 switching time. DC motor speed in discontinuous mode was 165 rad / s in 3 different switching times. It was observed that the oscillations in acceleration decreased as the switching times increase. In the 0.9 modulation index, the motor current at continuous mode reached a maximum value of 450 A at 0.07 s, while the motor speed reached 165 rad / s in 1 s. In the 0.7 modulation index, the motor current reached a maximum value of 375 A at 0.06 s, while the motor speed reached 142 rad / s in 1 s. In the 0.5 modulation index, the motor current reached a maximum value of 330 A at 0.05 s, while the motor speed reached 127 rad / s in 1 s. In the 0.9 modulation index, the engine torque at continuous mode reached 750Nm at 0.07s, while the maximum engine speed reaches 165 rad / s. In the 0.7 modulation index, the engine torque reached 675Nm at 0.06s, while the maximum engine speed reached 142 rad / s. In the 0.5 modulation index, the maximum value of the engine torque reached 600Nm at 0.05s, while the maximum engine speed reached 127 rad / s. When the obtained results were observed, dc motor torque, current, and speed were controlled in the desired way by using the new method in continuous and discontinuous mode.

References

- [1] J. Rashed, "Simulation of speed control for separately excited dc motor utilizing fuzzy logic controller," *University of Thi-Qar Journal for Engineering Sciences*, vol. 10, no. 1, p. 141–146. <http://jeng.utq.edu.iq/index.php/main/article/view/232>.
- [2] A. Abdullah and M. Ali, "Direct torque control of im using pid controller," *International Journal of Electrical and Computer Engineering (IJECE)*, vol. 10, no. 1, p. 617–625. DOI: [10.11591/ijece.v10i1.pp617-625](https://doi.org/10.11591/ijece.v10i1.pp617-625)
- [3] B. Gopal, E. Shivakumar, and H. Ramesh, "Design of deep learning controller for vector controlled induction motor drive," in *Data Engineering and Communication Technology*, p. 639–647, Singapore: Springer. DOI: [10.1007/978-981-15-1097-7_53](https://doi.org/10.1007/978-981-15-1097-7_53)
- [4] H. Bouyahi, K. Ben Smida, and A. Khedher, "Experimental study of pwm strategy effect on acoustic noise generated by inverter-fed induction machine," *International Transactions on Electrical Energy Systems*, vol. 12249. DOI: [10.1002/2050-7038.12249](https://doi.org/10.1002/2050-7038.12249)
- [5] A. Perry, G. Feng, Y. Liu, and P. Sen, "A design method for pi-like fuzzy logic controllers for dc-dc converter," *IEEE Transactions on Industrial Electronics*, vol. 54, no. 5, pp. 2688–2696,. DOI: [10.1109/TIE.2007.899858](https://doi.org/10.1109/TIE.2007.899858)

- [6] A. Chlahawi, "Genetic algorithm error criteria as applied to pid controller dc-dc buck converter parameters: an investigation," *IOP Conference Series: Materials Science and Engineering*, vol. 671, no. 1, p. 012032. DOI: [10.1088/1757-899X/671/1/012032](https://doi.org/10.1088/1757-899X/671/1/012032)
- [7] S. Devi Vidhya and M. Balaji, "Hybrid fuzzy pi controlled multi-input dc/dc converter for electric vehicle application," *Automatika*, vol. 61, no. 1, p. 79–91. DOI: [10.1080/00051144.2019.1684038](https://doi.org/10.1080/00051144.2019.1684038)
- [8] M. Muruganandam and M. Madheswaran, "Performance analysis of fuzzy logic controller based dc-dc converter fed dc series motor," in *2009 Chinese Control and Decision Conference*, p. 1635–1640. DOI: [10.1109/CCDC.2009.5192235](https://doi.org/10.1109/CCDC.2009.5192235)
- [9] A. Panda, S. Kahare, and S. Gawre, "Dsp tms320f28377s based speed control of dc motor," in *2020 IEEE International Students' Conference on Electrical, Electronics and Computer Science (SCEECS)*, p. 1–4. DOI: [10.1109/SCEECS48394.2020.133](https://doi.org/10.1109/SCEECS48394.2020.133)
- [10] E. Can, "Application of adaptive neuro-fuzzy logic method of noised electrical signals for correction," *Tecciencia*, vol. 15, no. 28, pp. 1–13, 2020. DOI: [10.18180/tecciencia.28.1](https://doi.org/10.18180/tecciencia.28.1)
- [11] Y. Sahin and N. Ting, "Soft switching passive snubber cell for family of pwm dc-dc converters," *Electrical Engineering*, vol. 100, no. 3, p. 1785–1796. DOI: [10.1007/s00202-017-0655-7](https://doi.org/10.1007/s00202-017-0655-7)
- [12] N. S. Ting, I. Aksoy, and Y. Sahin, "Zvt-pwm dc-dc boost converter with active snubber cell," *IET Power Electronics*, vol. 10, no. 2, p. 251–260. DOI: [10.1049/iet-pe1.2015.1052](https://doi.org/10.1049/iet-pe1.2015.1052)
- [13] M. Akhil, V. Aishwarya, and K. Sheela, "An improved sepic-based single switch buck-boost pfc converter fed brushless dc motor drive," *Materials Today: Proceedings*, vol. 24, p. 1855–1864. DOI: [10.1016/j.matpr.2020.03.610](https://doi.org/10.1016/j.matpr.2020.03.610)
- [14] A. Soriano-Sánchez, M. Rodríguez-Licea, F. Pérez-Pinal, and J. Vázquez-López, "Fractional-order approximation and synthesis of a pid controller for a buck converter," *Energies*, vol. 13, no. 3, p. 629. DOI: [10.3390/en13030629](https://doi.org/10.3390/en13030629)
- [15] R. Araria, K. Negadi, M. Boudiaf, and F. Marignetti, "Non-linear control of dc-dc converters for battery power management in electric vehicle application," *Przełąd Elektrotechniczny*, vol. 96. DOI: [10.15199/48.2020.03.20](https://doi.org/10.15199/48.2020.03.20)
- [16] M. Kavitha and V. Sivachidambaranathan, "Power factor correction in fuzzy based brushless dc motor fed by bridgeless buck boost converter," in *2017 International Conference on Computation of Power, Energy Information and Commuincation (ICCPEIC)*, p. 549–553, IEEE. DOI: [10.1109/ICCPEIC.2017.8290426](https://doi.org/10.1109/ICCPEIC.2017.8290426)
- [17] S. Yahyazadeh, M. Khaleghi, S. Farzamkia, and A. Khoshkbar-Sadigh, "A new structure of bidirectional dc-dc converter for electric vehicle applications," in *2020 11th Power Electronics, Drive Systems, and Technologies Conference (PEDSTC)*, p. 1–6. DOI: [10.1109/PEDSTC49159.2020.9088414](https://doi.org/10.1109/PEDSTC49159.2020.9088414)
- [18] C. Erol, "Doğrusal darbe genişlik modülasyonlu igt anahtarların kontrol ettiği dc motor," *Erzincan Üniversitesi Fen Bilimleri Enstitüsü Dergisi*, vol. 10, no. 2, p. 314–320. DOI: [10.18185/erzifbed.346878](https://doi.org/10.18185/erzifbed.346878), <https://dergipark.org.tr/en/download/article-file/388337>.
- [19] E. Can, "The load performance of multi-level alternating voltage provided by upgrade effect," *Jurnal Keju-ruteraan*, vol. 31, no. 2. DOI: [10.17576/jkukm-2019-31\(2\)-09](https://doi.org/10.17576/jkukm-2019-31(2)-09)
- [20] E. Can, "Energy transformation without using filter on high resistive load," *Engineering Review*, vol. 40, no. 1, p. 39–47. DOI: [10.30765/er.40.1.0](https://doi.org/10.30765/er.40.1.0), <https://hrcak.srce.hr/232825>.
- [21] E. Can and H. Sayan, "The increasing harmonic effects of sspwm multilevel inverter controlling load currents investigated on modulation index," *Tehnicki Vjesnik*, vol. 24, no. 2, p. 397–404. DOI: [10.17559/TV-20151020134629](https://doi.org/10.17559/TV-20151020134629)

- [22] A. AKSÖZ and A. SAYGIN, "Decreasing the cogging torque using virtual positive impedance based active damping control method for pmsms," *International Journal of Computational and Experimental Science and Engineering*, vol. 5, no. 1, p. 43-47. DOI: [10.22399/ijcesen.522865](https://doi.org/10.22399/ijcesen.522865)

